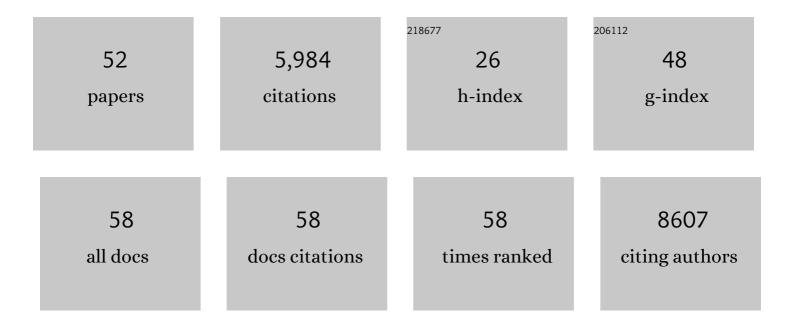
Julian Michael Tyszka

List of Publications by Year in descending order

Source: https://exaly.com/author-pdf/2080339/publications.pdf

Version: 2024-02-01



#	Article	IF	CITATIONS
1	The autism brain imaging data exchange: towards a large-scale evaluation of the intrinsic brain architecture in autism. Molecular Psychiatry, 2014, 19, 659-667.	7.9	1,882
2	Agenesis of the corpus callosum: genetic, developmental and functional aspects of connectivity. Nature Reviews Neuroscience, 2007, 8, 287-299.	10.2	687
3	Personal space regulation by the human amygdala. Nature Neuroscience, 2009, 12, 1226-1227.	14.8	324
4	Myocardial iron loading in transfusion-dependent thalassemia and sickle cell disease. Blood, 2004, 103, 1934-1936.	1.4	315
5	A high-resolution probabilistic in vivo atlas of human subcortical brain nuclei. Scientific Data, 2018, 5, 180063.	5.3	312
6	Largely Typical Patterns of Resting-State Functional Connectivity in High-Functioning Adults with Autism. Cerebral Cortex, 2014, 24, 1894-1905.	2.9	188
7	Contributions of the Amygdala to Reward Expectancy and Choice Signals in Human Prefrontal Cortex. Neuron, 2007, 55, 545-555.	8.1	183
8	Statistical diffusion tensor histology reveals regional dysmyelination effects in the shiverer mouse mutant. NeuroImage, 2006, 29, 1058-1065.	4.2	164
9	Intact Bilateral Resting-State Networks in the Absence of the Corpus Callosum. Journal of Neuroscience, 2011, 31, 15154-15162.	3.6	157
10	Neural Correlates of Specific and General Pavlovian-to-Instrumental Transfer within Human Amygdalar Subregions: A High-Resolution fMRI Study. Journal of Neuroscience, 2012, 32, 8383-8390.	3.6	148
11	Three-dimensional, time-resolved (4D) relative pressure mapping using magnetic resonance imaging. Journal of Magnetic Resonance Imaging, 2000, 12, 321-329.	3.4	142
12	In vivo delineation of subdivisions of the human amygdaloid complex in a highâ€resolution group template. Human Brain Mapping, 2016, 37, 3979-3998.	3.6	132
13	Idiosyncratic Brain Activation Patterns Are Associated with Poor Social Comprehension in Autism. Journal of Neuroscience, 2015, 35, 5837-5850.	3.6	130
14	Differentiation of benign and malignant adnexal masses: relative value of gray-scale, color Doppler, and spectral Doppler sonography American Journal of Roentgenology, 1995, 164, 381-386.	2.2	125
15	Parceling of mesial frontal motor areas during ideation and movement using functional magnetic resonance imaging at 1.5 tesla. Annals of Neurology, 1994, 35, 746-749.	5.3	120
16	Magnetic resonance microscopy: recent advances and applications. Current Opinion in Biotechnology, 2005, 16, 93-99.	6.6	118
17	The Immune Response to Herpes Simplex Virus Type 1 Infection in Susceptible Mice Is a Major Cause of Central Nervous System Pathology Resulting in Fatal Encephalitis. Journal of Virology, 2008, 82, 7078-7088.	3.4	110
18	The human amygdala parametrically encodes the intensity of specific facial emotions and their categorical ambiguity. Nature Communications, 2017, 8, 14821.	12.8	106

#	Article	IF	CITATIONS
19	Regional requirements for Dishevelled signaling during Xenopusgastrulation: separable effects on blastopore closure, mesendoderm internalization and archenteron formation. Development (Cambridge), 2004, 131, 6195-6209.	2.5	73
20	A specific hypoactivation of right temporo-parietal junction/posterior superior temporal sulcus in response to socially awkward situations in autism. Social Cognitive and Affective Neuroscience, 2015, 10, 1348-1356.	3.0	67
21	Distinct Contributions of Ventromedial and Dorsolateral Subregions of the Human Substantia Nigra to Appetitive and Aversive Learning. Journal of Neuroscience, 2015, 35, 14220-14233.	3.6	62
22	High efficiency, low distortion 3D diffusion tensor imaging with variable density spiral fast spin echoes (3D DW VDS RARE). NeuroImage, 2010, 49, 1510-1523.	4.2	45
23	Intrinsic Functional Connectivity of the Brain in Adults with a Single Cerebral Hemisphere. Cell Reports, 2019, 29, 2398-2407.e4.	6.4	44
24	The Claustrum and Insula in Microcebus murinus: A High Resolution Diffusion Imaging Study. Frontiers in Neuroanatomy, 2012, 6, 21.	1.7	37
25	Navigated single-voxel proton spectroscopy of the human liver. Magnetic Resonance in Medicine, 1998, 39, 1-5.	3.0	34
26	Evidence for model-based encoding of Pavlovian contingencies in the human brain. Nature Communications, 2019, 10, 1099.	12.8	31
27	Brain Differences in the Prefrontal Cortex, Amygdala, and Hippocampus in Youth with Congenital Adrenal Hyperplasia. Journal of Clinical Endocrinology and Metabolism, 2020, 105, 1098-1111.	3.6	31
28	Causal mapping of emotion networks in the human brain: Framework and initial findings. Neuropsychologia, 2020, 145, 106571.	1.6	22
29	Effect of Inversion Recovery Fat Suppression on Hepatic R2* Quantitation in Transfusional Siderosis. American Journal of Roentgenology, 2015, 204, 625-629.	2.2	18
30	High resolution magnetic resonance imaging of the brain in the dy/dy mouse with merosin-deficient congenital muscular dystrophy. Neuromuscular Disorders, 2000, 10, 292-298.	0.6	17
31	Distinct prediction errors in mesostriatal circuits of the human brain mediate learning about the values of both states and actions: evidence from high-resolution fMRI. PLoS Computational Biology, 2017, 13, e1005810.	3.2	16
32	Phase-contrast cine MR angiography detection of thoracic aortic dissection. International Journal of Cardiovascular Imaging, 2000, 16, 461-470.	0.6	15
33	Quantification of B0 homogeneity variation with head pitch by registered three-dimensional field mapping. Journal of Magnetic Resonance, 2002, 159, 213-218.	2.1	14
34	New tools for visualization and analysis of morphogenesis in spherical embryos. Developmental Dynamics, 2005, 234, 974-983.	1.8	14
35	No strong evidence that social network index is associated with gray matter volume from a data-driven investigation. Cortex, 2020, 125, 307-317.	2.4	14
36	T2-weighted μMRI and Evoked Potential of the Visual System Measurements During the Development of Hypomyelinated Transgenic Mice. Neurochemical Research, 2007, 32, 159-165.	3.3	11

Julian Michael Tyszka

#	Article	IF	CITATIONS
37	A uniplanar three-axis gradient set for in vivo magnetic resonance microscopy. Journal of Magnetic Resonance, 2009, 200, 38-48.	2.1	11
38	Volumetric multishot echo-planar spectroscopic imaging. Magnetic Resonance in Medicine, 2001, 46, 219-227.	3.0	10
39	Microstructural properties within the amygdala and affiliated white matter tracts across adolescence. NeuroImage, 2021, 243, 118489.	4.2	10
40	Restructuring of amygdala subregion apportion across adolescence. Developmental Cognitive Neuroscience, 2021, 48, 100883.	4.0	8
41	Highâ€field diffusion MR histology: Imageâ€based correction of eddyâ€current ghosts in diffusionâ€weighted rapid acquisition with relaxation enhancement (DWâ€RARE). Magnetic Resonance in Medicine, 2009, 61, 728-733.	3.0	7
42	Reorganization of the Social Brain in Individuals with Only One Intact Cerebral Hemisphere. Brain Sciences, 2021, 11, 965.	2.3	6
43	Navigated Single-Voxel Short-Echo-Time Proton Spectroscopy of Moving Objects. Journal of Magnetic Resonance Series B, 1996, 112, 302-306.	1.6	4
44	DOSE TITRATION OF DEFERASIROX IRON CHELATION THERAPY BY MAGNETIC RESONANCE IMAGING FOR CHRONIC IRON STORAGE DISEASE IN THREE ADULT RED BALD-HEADED UAKARI (CACAJAO CALVUS) Tj ETQqO O	0 rg .B T /C	over\$ock 10 Tf
45	Associations between testosterone, estradiol, and androgen receptor genotype with amygdala subregions in adolescents. Psychoneuroendocrinology, 2022, 137, 105604.	2.7	3
46	Videoâ€evoked fMRI BOLD responses are highly consistent across different data acquisition sites. Human Brain Mapping, 2022, 43, 2972-2991.	3.6	3
47	How important is the corpus callosum in resting-state networks?. Future Neurology, 2012, 7, 231-234.	0.5	1
48	Compact brain MRI. Nature Biomedical Engineering, 2021, 5, 201-202.	22.5	1
49	Caltech Conte Center, a multimodal data resource for exploring social cognition and decision-making. Scientific Data, 2022, 9, 138.	5.3	1
50	Related Methods for Three-Dimensional Imaging. , 2006, , 607-626.		0
51	New tools for visualization and analysis of morphogenesis in spherical embryos. Developmental Dynamics, 2006, 235, spc1-spc1.	1.8	0
52	Motion-sensitive 3-D optical coherence microscope operating at 1300 nm for the visualization of early frog development. , 2007, , .		0